PAPER

Integrating electric field modeling and pre-tDCS behavioral performance to predict the individual tDCS effect on visual crowding

To cite this article: Luyao Chen *et al* 2023 *J. Neural Eng.* **20** 056019

IOP Publishing J. Neural Eng. 20 (2023) 056019 https://doi.org/10.1088/1741-2552/acfa8c

Journal of Neural Engineering

RECEIVED
12 May 2023

REVISED
8 September 2023

ACCEPTED FOR PUBLICATION
15 September 2023

PUBLISHED
26 September 2023

PAPER

Integrating electric field modeling and pre-tDCS behavioral performance to predict the individual tDCS effect on visual crowding

Luyao Chen[1,2,3,4], **Guanpeng Chen**[1,3,4,5], **Xizi Gong**[1,3,4,5] **and Fang Fang**[1,2,3,4,5,*]

[1] School of Psychological and Cognitive Sciences and Beijing Key Laboratory of Behavior and Mental Health, Peking University, Beijing 100871, People's Republic of China
[2] Beijing Academy of Artificial Intelligence, Beijing 100084, People's Republic of China
[3] IDG/McGovern Institute for Brain Research, Peking University, Beijing 100871, People's Republic of China
[4] Key Laboratory of Machine Perception (Ministry of Education), Peking University, Beijing 100871, People's Republic of China
[5] Peking-Tsinghua Center for Life Sciences, Peking University, Beijing 100871, People's Republic of China
[*] Author to whom any correspondence should be addressed.

E-mail: ffang@pku.edu.cn

Keywords: transcranial direct current stimulation (tDCS), high-definition tDCS (HD-tDCS), visual crowding, inter-individual variability, focality

Supplementary material for this article is available online

Abstract

Objective. Transcranial direct current stimulation (tDCS) has been broadly used to modulate brain activity with both bipolar and high-definition montages. However, tDCS effects can be highly variable. In this work, we investigated whether the variability in the tDCS effects could be predicted by integrating individualized electric field modeling and individual pre-tDCS behavioral performance. *Approach.* Here, we first compared the effects of bipolar tDCS and 4 × 1 high-definition tDCS (HD-tDCS) with respect to the alleviation of visual crowding, which is the inability to identify targets in the presence of nearby flankers and considered to be an essential bottleneck of object recognition and visual awareness. We instructed subjects to perform an orientation discrimination task with both isolated and crowded targets in the periphery and measured their orientation discrimination thresholds before and after receiving 20 min of bipolar tDCS, 4 × 1 HD-tDCS, or sham stimulation over the visual cortex. Individual anatomically realistic head models were constructed to simulate tDCS-induced electric field distributions and quantify tDCS focality. Finally, a multiple linear regression model that used pre-tDCS behavioral performance and tDCS focality as factors was used to predict post-tDCS behavioral performance. *Main results.* We found that HD-tDCS, but not bipolar tDCS, could significantly alleviate visual crowding. Moreover, the variability in the tDCS effect could be reliably predicted by subjects' pre-tDCS behavioral performance and tDCS focality. This prediction model also performed well when generalized to other two tDCS protocols with a different electrode size or a different stimulation intensity. *Significance.* Our study links the variability in the tDCS-induced electric field and the pre-tDCS behavioral performance in a visual crowding task to the variability in post-tDCS performance. It provides a new approach to predicting individual tDCS effects and highlights the importance of understanding the factors that determine tDCS effectiveness while developing more robust protocols.

1. Introduction

Transcranial direct current stimulation (tDCS) is a non-invasive neuromodulation method that delivers a weak and constant current to cortical areas via electrodes attached to the scalp surface. Conventional bipolar tDCS uses two large rectangular pads and leads to diffuse brain modulation [1–3]. To improve stimulation focality and accuracy, high-definition tDCS (HD-tDCS) was introduced, which uses four

return electrodes surrounding a stimulation electrode [1–3]. Both the tDCS protocols have been widely used to treat neuropsychiatric disorders [4–6], and to modulate motor [7–9], sensory [10–12], and cognitive functions [9, 13].

Despite showing promise for numerous applications, tDCS has received considerable criticism regarding the fact of ubiquitous inter-individual variability in its modulatory effects [14–16]. This makes it challenging for researchers to replicate tDCS outcomes and therefore limits its potential use cases. It has been suggested that the prevalence of inter-individual variability in the effects of tDCS may be explained by individual differences in pre-tDCS behavioral performance [17–20] or biological parameters [21–25]. For example, patients' pre-tDCS cognitive and language performance may predict the effects of tDCS on primary progressive aphasia [17]. Several depression severity-related factors have been identified as potential clinical predictors of the response to tDCS in depressed patients [18]. Meanwhile, computational modeling studies have shown that anatomical factors, such as brain atrophy [21], cerebrospinal fluid (CSF) thickness [22], uncertain head tissue conductivity [23], and the anisotropic conductivity of head tissues [24, 25] influence the strength and focality of the stimulation-induced electric field in the brain. Apart from qualitatively clarifying the influence of these factors, using them to quantitatively predict individual tDCS effects is of great significance. Previous prediction models focused mainly on the biological parameters such as gray matter (GM) density [26], white matter integrity [27], and head volume [28], but ignored the role of tDCS-induced electric field in predicting post-tDCS behavioral performance. In addition, these models mainly focused on bipolar tDCS, but did not test their generalizability to other tDCS protocols.

In the current study, we investigated whether the combination of individual electric field modeling and pre-tDCS behavioral performance can predict individual post-tDCS behavioral performance. Here we adopted visual crowding as the experimental paradigm to test the effectiveness of our prediction model for tDCS. Visual crowding is the inability to identify targets in the presence of nearby flankers (illustrated in figure 1). This is a ubiquitous phenomenon in spatial vision that has been observed in many stimuli, including oriented gratings, letters, and faces [29]. Visual crowding is considered as an essential bottleneck of object recognition and visual awareness [29, 30]. Alleviating the visual crowding effect can improve peripheral vision and may therefore have potential clinical implications for patients with visual deficits such as macular degeneration [30] and amblyopia [31]. It has been demonstrated that offline bipolar tDCS on posterior parietal cortex is effective in alleviating visual crowding [32]. Notably,

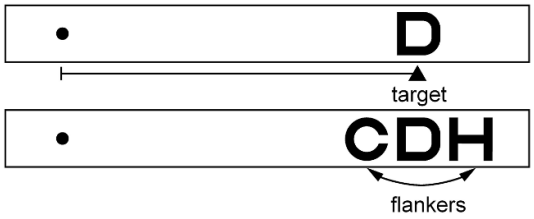

Figure 1. Schematic description of visual crowding. When fixating at the black dot on the left, identification of the target 'D' is easy in the isolated condition (top). However, in the crowded condition, i.e. when the target 'D' is presented with the nearby flankers 'C' and 'H', identification becomes difficult or impossible (bottom).

event-related potential and functional magnetic resonance imaging studies on the neural mechanisms of visual crowding have shown that early visual cortex (i.e. V1 and V2) plays an important role in visual crowding [33–37]. Therefore, we speculate that tDCS on early visual cortex may also be able to alleviate visual crowding by modulating the related neural activities.

In this work, we conducted a single-blind sham-controlled study to investigate the effects of both bipolar tDCS and 4 × 1 HD-tDCS on visual crowding. To demonstrate the visual crowding effect, subjects were instructed to perform an orientation discrimination task under two conditions: with isolated and crowded targets. The anodal electrode of tDCS was placed over early visual cortex. Furthermore, we constructed realistic head models to simulate the tDCS-induced electric field and calculate the stimulation focality of each subject. We found that HD-tDCS was effective in alleviating the visual crowding effect, while the modulatory effect of bipolar tDCS was not significant. More importantly, we found that the inter-individual variability of the tDCS effect on visual crowding could be predicted by a model including both individual stimulation focality and pre-tDCS behavioral performance as factors. Finally, the proposed prediction model could be generalized to other two tDCS protocols that used a different electrode size or a different stimulation intensity.

2. Methods

2.1. Participants

A total of 75 subjects (31 males, 19–30 years old) were recruited and randomly assigned to one of five groups: a HD-1 mA tDCS group (where subjects received HD-tDCS at a stimulation intensity of 1 mA, $n = 15$, 4 males), a bipolar-25 tDCS group (where subjects received bipolar tDCS at a stimulation intensity of 1 mA, electrode size = 25 cm^2, $n = 15$, 8 males), a HD-2 mA tDCS group (where subjects received HD-tDCS at a stimulation intensity

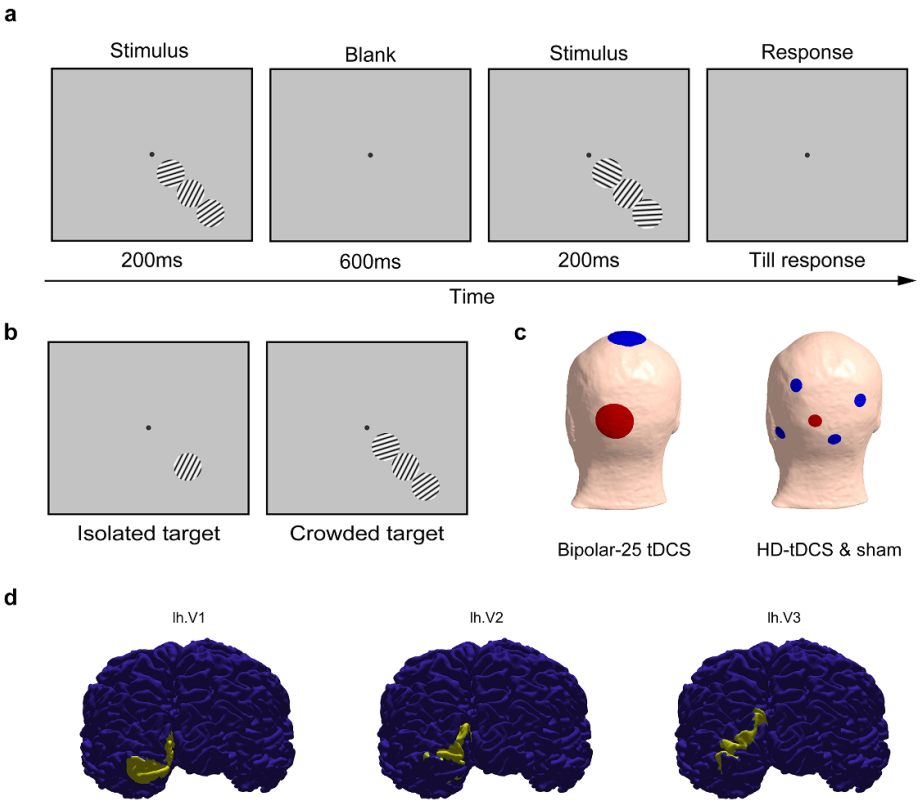

Figure 2. Experimental design and tDCS montages. (a) Schematic description of an orientation discrimination trial with the crowded targets. (b) Visual stimuli used in the isolated and crowded conditions. (c) tDCS montages for subjects with visual stimuli appearing in the lower-right visual quadrant. Black dot represents the fixation point. (d) V1, V2, and V3 based on the HCP-MMP atlas.

of 2 mA, $n = 15$, 7 males), a bipolar-8 tDCS group (where subjects received bipolar tDCS at a stimulation intensity of 1 mA, electrode size = 8 cm^2, $n = 15$, 6 males), and a sham stimulation group (where subjects received a sham stimulation, $n = 15$, 6 males). The first two tDCS protocols were commonly used in previous studies, while the last two tDCS groups were designed to test the generalization of the prediction model based on the first three groups to different tDCS protocols. All subjects were right-handed, reported normal or corrected-to-normal vision, and had no known neurological or visual disorders. Written informed consent was obtained from all subjects. All experimental procedures were approved by the human subject review committee of Peking University.

2.2. Stimuli, task design, and apparatus

Visual stimuli and task design were similar to experiment 1 of our previous study [32]. The experiment consisted of three phases: a pre-tDCS behavioral performance test (Pre), an offline tDCS phase, and a post-tDCS behavioral performance test (Post). The three phases were conducted continuously with one phase carried out immediately after the preceding one. In the tDCS phase, subjects received 20 min of bipolar tDCS, 1 × 4 HD-tDCS, or sham stimulation. Before and after tDCS, subjects were instructed to perform an orientation discrimination task with both isolated and crowded targets (stimulus position: either in the lower-left or lower-right visual quadrant; figures 2(a) and (b)). These two tasks are hereafter referred to as the 'isolated condition' and 'crowded condition' respectively. Ten QUEST staircases [38] of 40 trials, with five staircases for each condition, were completed alternately between the two conditions. Visual stimuli were displayed on an Cambridge Research Systems—Display++ LCD Monitor 32 inch monitor (spatial resolution: 1920 × 1080; refresh rate: 120 Hz) with a gray background (luminance: 34.8 cd m^{-2}). Subject head positions were stabilized with a head and chin rest, and the viewing distance was 70 cm. During the experiments, subjects were asked to maintain their fixation on a black dot at the center of the display, and their eye positions were monitored with an Eyelink 1000 Plus eye-tracking system.

2.3. tDCS protocol

tDCS was applied using a battery-powered apparatus (StarStim32; Neuroelectrics Inc.). We used two saline-soaked sponge electrodes for the bipolar tDCS groups and five conductive gel-covered PISTIM Ag/AgCl electrodes for the HD-tDCS groups. The anodal electrode used for all tDCS groups was placed over the visual cortex of the hemisphere contralateral

to the visual stimulus, i.e. at O1 for subjects with target gratings presented in the lower-right quadrant, and at O2 for subjects with target gratings presented in the lower-left quadrant. The cathodal electrode used for bipolar tDCS groups was placed at Cz. For the HD-tDCS groups, the four return electrodes were placed either at P9, Iz, PO3, and P4 if the anodal electrode was placed at O1, or at P10, Iz, PO4, and P3 if the anodal electrode was placed at O2. All positions were determined according to the international 10–10 electroencephalogram system (figure 2(c)). During tDCS, the impedance was kept below 10 KΩ. For the tDCS groups, the current was ramped up to a specific intensity (2 mA for the HD-2 mA tDCS group, and 1 mA for the other groups) over 30 s, held constant for 20 min, then ramped back down to zero over 30 s. For the sham group, the current was ramped up to 1 mA over 30 s then held constant and switched off in next 5 s.

2.4. MRI data acquisition

To perform individual simulation of the tDCS-induced electric field, T1-weighted MRI data were collected using a 3 T Siemens Prisma MRI scanner with a 3D-MPRAGE sequence (TR = 2530 ms, TE = 2.98 ms, voxel size: $1 \times 1 \times 1$ mm^3). Forty-two subjects (HD-1 mA group: 9, bipolar-25 group: 13, bipolar-8 group: 9, HD-2 mA group: 11) participated in the MRI data acquisition procedure.

2.5. Electric field simulation

We used SimNIBS version 3.2 to calculate the distribution of the electric field induced by tDCS using the finite element method [39, 40]. Individual head models were reconstructed from the T1-weighted structural MRI data for each subject. Scalp, skull, CSF, GM, and white matter were segmented automatically, and the corresponding electric conductivity values were set as 0.465 S m^{-1}, 0.01 S m^{-1}, 1.654 S m^{-1}, 0.275 S m^{-1}, and 0.126 S m^{-1}, respectively [41]. PISTIM electrodes were modeled as a 2 mm thick cylinder with a 2 mm thick conductive gel layer. The electric conductivity values of the electrode and gel were 5.8×10^7 S m^{-1} and 0.3 S m^{-1} [42], respectively. The sponge electrodes were modeled as a 1 mm-thick rubber pad enclosed by a 3 mm-thick sponge. The electric conductivity values of the rubber pad and soaked sponge were 29.4 S m^{-1} [43] and 1.4 S m^{-1} [42], respectively. The peak electric field strength and focality were computed from the simulation results *per* subject and stimulation protocol. Focality was quantified as the area of the GM region where the electric field strength exceeded 0.1 V m^{-1} across the whole brain in subject space [44]. Moreover, V1, V2, and V3 were defined for each subject by the HCP-MMP atlas [45]. Figure 2(d) showed V1, V2, and V3 of a subject in the bipolar-25 tDCS group. We further quantified the focality in V1 (referred to as focality-V1), V2 (referred to as focality-V2), and V3 (referred to as focality-V3) by calculating the area of the GM region where the electric field strength exceeded 0.1 V m^{-1} in V1, V2, and V3, respectively. Thus, a protocol with a smaller focality value would generate a more focal stimulation effect. To calculate the average electric field distributions and the deviations, simulation results were transformed into the fsaverage space [46–48].

2.6. Data analysis

We quantified subjects' pre-tDCS and post-tDCS behavioral performance as the mean threshold of the five QUEST staircases at Pre and Post, respectively. Subjects' behavioral performance improvement was calculated as: (pre-tDCS behavioral performance − post-tDCS behavioral performance)/pre-tDCS behavioral performance × 100%. We then compared the discrimination thresholds for the isolated and crowded conditions before and after tDCS across groups using a three-way analyses of variance (ANOVA) with condition (isolated and crowded) and test (i.e. Pre or Post) as within-subject factors, and the stimulation protocol (i.e. bipolar-25, HD-1 mA, or sham) as a between-subject factor. Further, to interpret the significant three-way interaction effect, we conducted two two-way ANOVAs for the isolated and crowded conditions separately. Planned two-tailed *t*-tests were then used to determine whether there were significant differences in threshold and/or improvement among the three tDCS groups in both conditions. For *t*-tests, we used a Bonferroni correction for multiple comparisons (corrected significance level: 0.05/3). We also noted that for each condition, there was no significant threshold difference at Pre among the three tDCS groups (one-way ANOVA, $p > 0.249$), or between the stimulation sides (O1 or O2) within each tDCS group (*t*-test, all *p* values > 0.05).

3. Results

3.1. Modulation of bipolar tDCS and HD-tDCS on visual crowding effect

We first assessed the effects of bipolar-25 and HD-1 mA tDCS on behavioral performance (i.e. orientation discrimination threshold) in the three groups. The crowding effect existed in all the three groups as the pre-tDCS threshold in the crowded condition was significantly higher than that in the isolated condition for all the groups (HD-1 mA tDCS, $t\ (14) = 8.94$, $p_{adj} < 0.001$; bipolar-25 tDCS, $t\ (14) = 5.91$, $p_{adj} < 0.001$; sham, $t\ (14) = 8.30$, $p_{adj} < 0.001$). Furthermore, we compared the effects of bipolar tDCS and 4 × 1 HD-tDCS on alleviating the visual crowding.

The three-way ANOVAs revealed that the main effect of condition and test were both statistically significant (condition: $F\ (1, 42) = 176.54$, $p < 0.001$, partial $\eta^2 = 0.808$; test: $F\ (1, 42) = 39.22$, $p < 0.001$, partial $\eta^2 = 0.483$), as well as the interaction effect

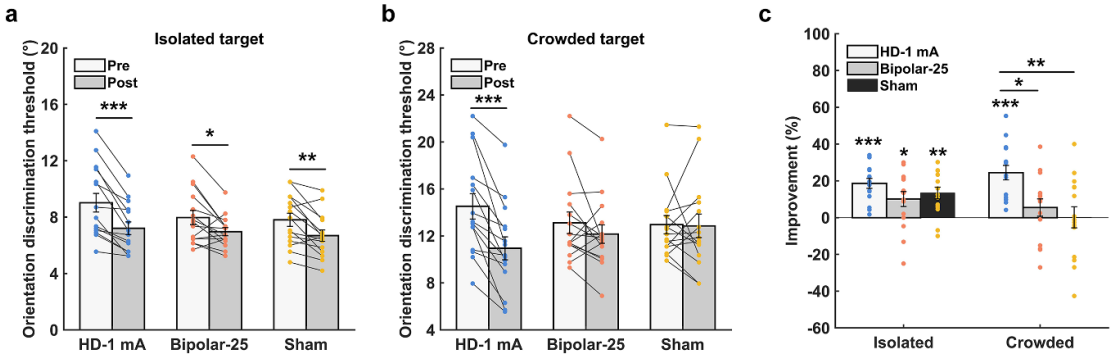

Figure 3. Effects of tDCS on visual crowding. (a) Orientation discrimination thresholds at Pre and Post in the isolated condition. (b) Orientation discrimination thresholds at Pre and Post in the crowded condition. (c) Percent improvement in orientation discrimination performance for all groups. Blue dots: subjects from the HD-1 mA group. Orange dots: subjects from the bipolar-25 group. Yellow dots: subjects from the sham stimulation group. $^{*}p < 0.05$, $^{**}p < 0.01$, $^{***}p < 0.001$. Error bars denote 1 SEM across subjects.

of stimulation protocol * test (F (2, 42) = 7.94, $p = 0.001$, partial $\eta^2 = 0.274$) and stimulation protocol * test * condition (F (2, 42) = 3.47, $p = 0.040$, partial $\eta^2 = 0.142$). Yet the main effect of stimulation protocol was not significant (F (2, 42) = 0.12, $p = 0.887$, partial $\eta^2 = 0.006$), not was the interaction effect of stimulation protocol * condition (F (2, 42) = 0.60, $p = 0.553$, partial $\eta^2 = 0.028$) or condition * test (F (1, 42) = 0.28, $p = 0.598$, partial $\eta^2 = 0.007$). Further, to interpret the significant three-way interaction effect, we conducted two two-way ANOVAs with test (i.e. Pre or Post) as a within-subject factor and stimulation protocol (i.e. bipolar-25, HD-1 mA, or sham) as a between-subject factor.

In the isolated condition, we found that the main effect of test was significant (F (1, 42) = 47.99, $p < 0.001$, partial $\eta^2 = 0.533$), but the main effect of stimulation protocol was not (F (2, 42) = 1.02, $p = 0.369$, partial $\eta^2 = 0.046$), and neither was the interaction between test and stimulation protocol (F (2,42) = 1.78, $p = 0.181$, partial $\eta^2 = 0.078$). Planned t-tests showed that for all three groups, the threshold measured at Post was significantly lower than that at Pre (HD-1 mA tDCS, t (14) = 5.44, $p_{adj} < 0.001$, Cohen's $d = 1.403$; bipolar-25 tDCS, t (14) = 2.79, $p_{adj} = 0.044$, Cohen's $d = 0.720$; sham, t (14) = 3.91, $p_{adj} = 0.005$, Cohen's $d = 1.008$); figure 3(a)). However, we found no significant improvement differences among the three stimulation groups (1-way ANOVA, F (2, 42) = 1.59, $p = 0.215$, $\eta^2 = 0.071$; planned t-tests, all $p_{adjs} > 0.283$). Thus, the performance improvement in both the HD-1 mA and the bipolar-25 tDCS groups could not be attributed to the electrical stimulation. Instead, we interpret this as simply a test-retest effect that was due to the training during the two tests.

In the crowded condition, we found that the main effect of test was significant (F (1, 42) = 14.52, $p < 0.001$, partial $\eta^2 = 0.257$), as was the interaction between test and stimulation protocol (F (2, 42) = 6.67, $p = 0.003$, partial $\eta^2 = 0.241$). However, the main effect of stimulation protocol was not significant (F (2, 42) = 0.03, $p = 0.974$, partial $\eta^2 = 0.001$). Planned t-tests showed that for the HD-1 mA tDCS group, the threshold measured at Post was significantly lower than that at Pre (HD-1 mA tDCS, t (14) = 5.48, $p_{adj} < 0.001$, Cohen's $d = 1.415$); in contrast, no such effect was observed for the bipolar-25 tDCS or sham groups (bipolar-25 tDCS, t (14) = 1.45, $p_{adj} = 0.510$; sham, t (14) = 0.12, $p_{adj} = 1$) (figure 3(b)). Moreover, planned t-tests after a one-way ANOVA (F (2, 42) = 6.97, $p = 0.002$, $\eta^2 = 0.249$) showed that the improvement in the HD-1 mA tDCS group was significantly higher than that in the bipolar-25 tDCS group (t (28) = 3.10, $p_{adj} = 0.013$, Cohen's $d = 1.131$) or in the sham group (t (28) = 3.50, $p_{adj} = 0.005$, Cohen's $d = 1.278$). Moreover, no significant improvement difference was found between the bipolar-25 tDCS and sham groups (t (28) = 0.72, $p_{adj} = 1$); figure 3(c). Since there was no significant difference in improvement among the three groups in the isolated condition, we conclude that subjects' orientation sensitivity *per se* could not be improved by tDCS. Thus, the performance improvement of the HD-1 mA tDCS group in the crowded condition resulted from the effect of HD-tDCS on alleviating the visual crowding effect.

At the group level, HD-1 mA tDCS, but not bipolar-25 tDCS, was effective in alleviating the visual crowding effect. However, we noted that there were large inter-individual variations in the subjects' improvement and post-tDCS performance in both groups. Therefore, we next attempted to develop a model capable of accounting for these variations.

3.2. Inter-individual variations in the electric field distribution

We investigated tDCS-induced electric field distributions in the brain by performing individual simulations based on realistic head models of subjects

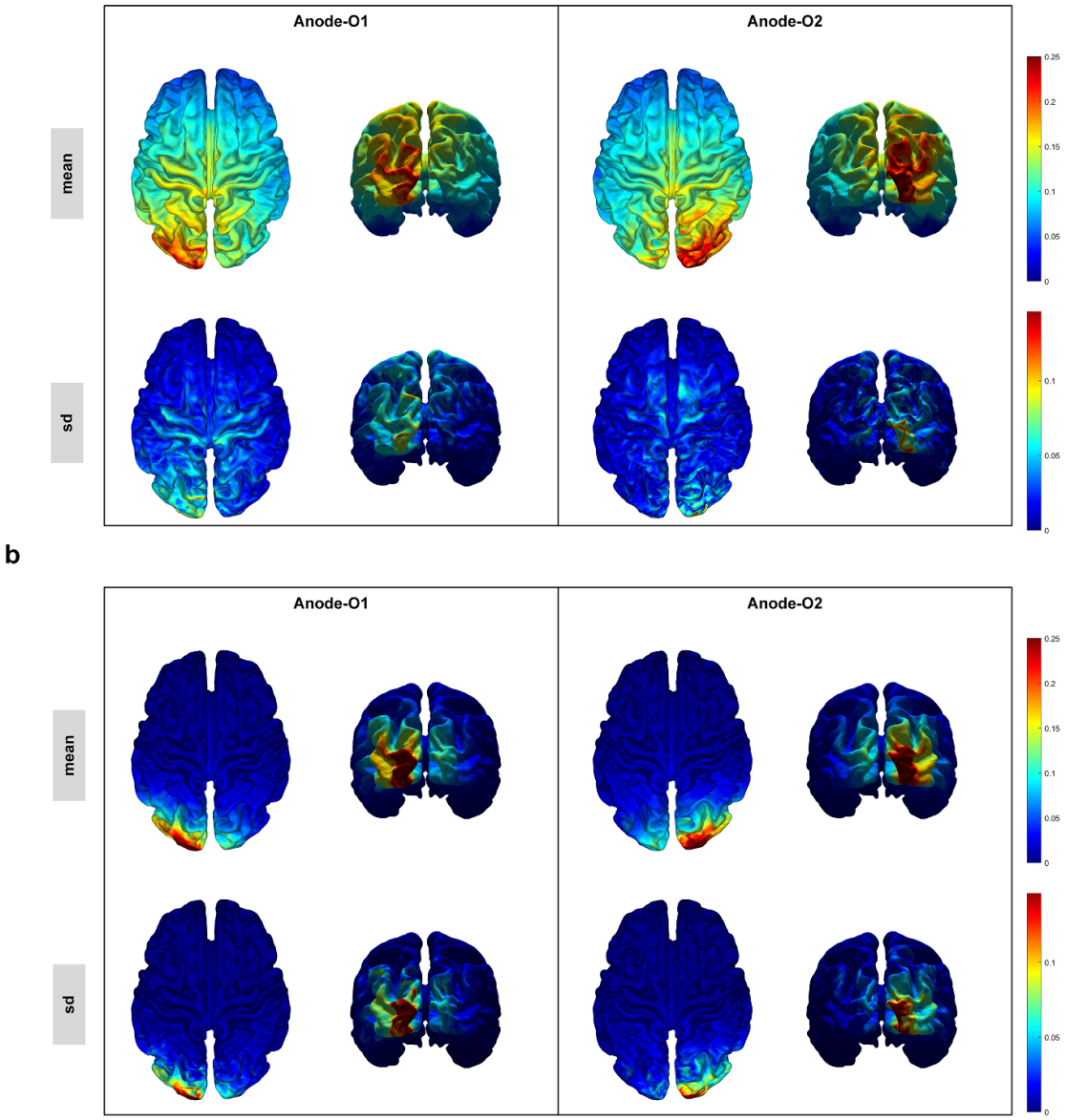

Figure 4. Inter-individual variations in the electric field distribution. (a) Simulation results in the bipolar-25 tDCS group. (b) Simulation results in the HD-1 mA tDCS group. Electric field averages (unit: V m^{-1}) and standard deviation for participants with the stimulation electrode fixed at O1 (left) or O2 (right). Simulations were performed on the individual brain and warped into fsaverage space.

from the bipolar-25 and HD-1 mA tDCS groups. Peak electric field strength and focality were computed for each subject. Results showed that peak electric field strength varied from 0.12 V m^{-1} to 0.78 V m^{-1} (mean ± SD: 0.46 ± 0.21 V m^{-1}) in the HD-1 mA group, and from 0.30 V m^{-1} to 0.55 V m^{-1} (mean ± SD: 0.40 ± 0.08 V m^{-1}) in the bipolar-25 tDCS group, respectively (supplementary figures 1 and 2). In addition, the focality of the electric field varied from 0.03 dm^2 to 2.19 dm^2 (mean ± SD: 1.12 ± 0.69 dm^2) in the HD-1 mA tDCS group, and from 3.36 dm^2 to 11.97 dm^2 (mean ± SD: 7.94 ± 2.69 dm^2) in the bipolar-25 tDCS group, respectively. To calculate the average electric field distributions and characterize the similarity of electric fields across subjects, simulation results were warped into the fsaverage space. The distribution of averaged electric field and the standard deviation are shown in figure 4 for both tDCS groups. These results demonstrate that in both groups, there were considerable inter-individual variations in the tDCS-induced electric field in the brain across subjects.

3.3. Integrating pre-tDCS behavioral performance with the focality of the electric field to predict the effect of tDCS on visual crowding

Thus far we found substantial variations in both the tDCS-modulated behavioral performance and the tDCS-induced electric field in the brain. Next, we put the behavioral and simulation results in a multiple linear regression model (hereafter referred to as the 'p-f model') using pre-tDCS behavioral performance

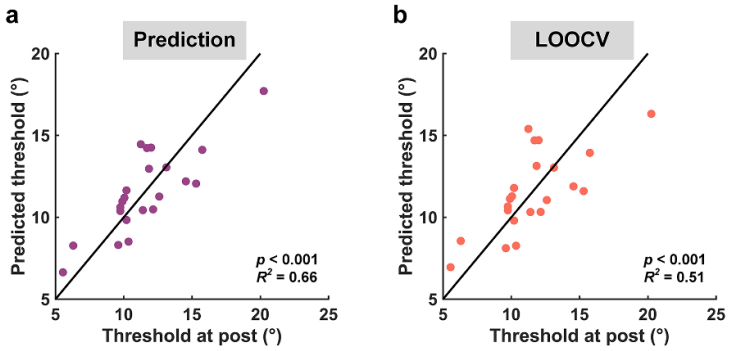

Figure 5. Model predictions. Scatterplots depict predicted post-tDCS performance plotted against observed experimental values. Each dot represents data from a single subject in the bipolar-25 and HD-1 mA tDCS groups. The diagonals indicate the line of perfect prediction (i.e. when predicted threshold is equal to observed threshold). Predicted thresholds were generated by (a) the prediction model, (b) cross-validation of the prediction model.

(hereafter referred to as the 'Pre-threshold') and focality as factors to determine whether the combination of inter-individual variations in pre-tDCS behavioral performance and tDCS-induced electric field among the subjects could account for the variability in the tDCS effect. We pooled data from the bipolar-25 and the HD-1 mA tDCS groups together because both protocols were designed to modulate visual cortex with similar tDCS mechanisms. Supplementary figure 3 shows post-tDCS behavioral performance as a function of pre-tDCS behavioral performance and electric field focality of the subjects. Compared with alternative models that contained only Pre-threshold or focality as a single factor, the p-f model exhibited the lowest Akaike's information criterion (AIC) score and the highest R^2 (table 1). The results of multiple linear regression analysis showed that the combination of the two factors explained 65.99% of the variance in post-tDCS behavioral performance ($R^2 = 0.66$, F (2, 19) = 18.43, $p < 0.001$; figure 5(a)). Moreover, both factors predicted the post-tDCS behavioral performance significantly (Pre-threshold, $beta = 0.59$, t (19) = 5.19, $p < 0.001$; focality, $beta = 0.40$, t (19) = 3.77, $p = 0.001$). Additionally, we analyzed the performance of the full model (the model contained the interaction term Pre-threshold * focality) and results showed that the interaction effect was not significant, nor was the effect of the factor focality (Pre-threshold, $beta = 0.48$, t (19) = 2.40, $p = 0.028$; focality, $beta = 0.08$, t (19) = 0.16, $p = 0.876$; Pre-threshold * focality, $beta = 0.02$, t (19) = 0.67, $p = 0.512$). This full model could explain 66.82% of the variance in post-tDCS behavioral performance ($R^2 = 0.67$, F (3, 18) = 12.08, $p < 0.001$). Considering the comparable R^2 but higher AIC value of the full model (AIC = 38.55, table 1), the p-f model was a more appropriate model. These results demonstrate that the inter-individual variability in the effect of tDCS on visual crowding induced by both protocols could be largely accounted for by variations in pre-tDCS behavioral performance and electric field focality of the subjects.

Table 1. Comparison of the R^2 and AIC values from different prediction models for the crowded condition.

Model	R^2	AIC
Pre-threshold + focality	0.66	35.69
Pre-threshold	0.41	44.98
Focality	0.18	52.07
Pre-threshold + focality + Pre-threshold * focality	0.67	38.55

3.4. Model validation and generalization

To obtain a more conservative estimate of the explained variance, we performed a leave-one-out cross-validation test of the data from the HD-1 mA and bipolar-25 groups. The training and test procedures were performed iteratively n times, with data from $n - 1$ subjects for training and data from the remaining subject for test. The results of this analysis (figure 5(b)) show that the p-f model still explained more than half (50.73%) of the variance in the tDCS groups ($R^2 = 0.51$, $p < 0.001$).

To investigate the generalizability of the p-f model to other tDCS protocols, we repeated the visual crowding experiment with two other tDCS protocols: bipolar-8 tDCS and HD-2 mA tDCS. In the crowded condition, we found that for the HD-2 mA group, the threshold measured at Post was significantly lower than that at Pre (HD-2 mA, t (14) = 3.81, $p_{adj} = 0.006$, Cohen's $d = 0.984$); in contrast, no such effect was observed for the bipolar-8 tDCS group (bipolar-8, t (14) = 1.2, $p_{adj} = 0.228$) (figure 6(a)). Moreover, planned t-tests after a one-way ANOVA (F (2, 42) = 4.19, $p = 0.022$, $\eta^2 = 0.166$) showed that the improvement in the HD-2 mA group was significantly higher than that in in the sham group (t (28) = 2.72, $p_{adj} = 0.033$, Cohen's $d = 0.992$), while no significant difference was observed between the

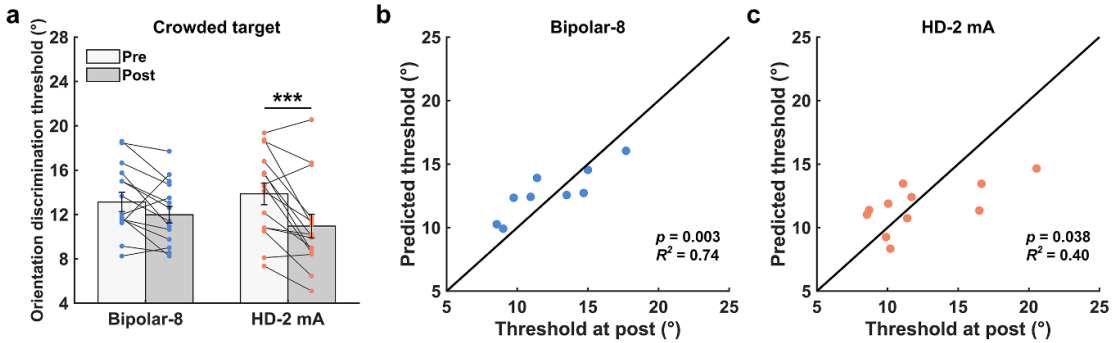

Figure 6. Generalizability of the prediction model. (a) Orientation discrimination thresholds of the bipolar-8 and HD-2 mA tDCS groups in the crowded condition. $^{***}p < 0.001$. Error bars denote 1 SEM across subjects. (b) and (c) Scatterplots depict predicted post-tDCS performance plotted against observed experimental values. Each dot represents data from (a) single subject in (b) the bipolar-8 tDCS group and (c) the HD-2 mA tDCS group.

Table 2. Comparison of different prediction models for the crowded condition.

Model	R^2	AIC	Sig_Pre	Sig_focality
Focality-w + Pre-threshold	0.66	35.69	***	**
Focality-V1 + Pre-threshold	0.59	39.56	***	**
Focality-V2 + Pre-threshold	0.58	40.55	***	*
Focality-V3 + Pre-threshold	0.51	43.68	***	n.s.

$^{*}p < 0.05$, $^{**}p < 0.01$, $^{***}p < 0.001$.

improvement in the bipolar-8 group and the sham group (t (28) = 0.90, $p_{adj} = 1$). Similar to the bipolar-25 and HD-1 mA tDCS groups, remarkable inter-individual variations in behavioral performance and tDCS modeling were also observed in the bipolar-8 and HD-2 mA groups (figure 6(a) and supplementary figures 4 and 5). We then used the p-f model derived from the data of the HD-1 mA and bipolar-25 tDCS groups to predict the post-tDCS performance of the subjects in the bipolar-8 and HD-2 mA tDCS groups. It was found that the p-f model could explain a considerable proportion of the variance in the post-tDCS performance of the bipolar-8 group ($R^2 = 0.74$, $p = 0.003$; figure 6(b)). For the HD-2 mA group, the prediction model explained approximately 39.53% of the variance and was statistically significant ($R^2 = 0.40$, $p = 0.038$; figure 6(c)). These findings demonstrate the robustness and generalizability of the p-f model, and suggest that it is a powerful tool for predicting the effects of various tDCS protocols.

3.5. ROI analysis on the modulated brain regions

To quantify what regions of the brain were being stimulated by tDCS protocols in this work, we separately applied focality-V1, focalty-V2, or focality-V3 together with pre-tDCS behavioral performance to the regression model (referred to as 'p-V1 model', 'p-V2 model', and 'p-V3 model', respectively) that aimed at predicting the post-tDCS behavioral performance. Results showed that the p-V1, p-V2, and p-V3 model could explain 59.45%, 57.59%, and 51.10% of the variance, respectively (the p-V1 model, $R^2 = 0.59$, F (2, 19) = 13.93, $p < 0.001$; the p-V2 model, $R^2 = 0.58$, F (2, 19) = 12.90, $p < 0.001$; the p-V3 model, $R^2 = 0.51$, F (2, 19) = 9.93, $p = 0.001$; supplementary figure 6, table 2). We found that the factors focality-V1 and focality-V2 significantly predicted the post-tDCS behavioral performance, while factor focality-V3 did not (The p-V1 model: pre-tDCS threshold, $beta = 0.56$, t (19) = 4.55, $p < 0.001$; focality-V1, $beta = 0.12$, t (19) = 2.98, $p = 0.008$. The p-V2 model: pre-tDCS threshold, $beta = 0.57$, t (19) = 4.55, $p < 0.001$; focality-V2, $beta = 0.15$, t (19) = 2.77, $p = 0.012$. The p-V3 model: pre-tDCS threshold, $beta = 0.58$, t (19) = 4.24, $p < 0.001$; focality-V3, $beta = 0.19$, t (19) = 2.03, $p = 0.057$. Table 2). These results demonstrate that the V1 and V2 are likely to be the functional regions that are responsible for the crowding effect, which are consistent with previous studies concerning the neural mechanism of visual crowding [33–36].

4. Discussion

In this work, we demonstrate that variability in tDCS-induced modulation of visual crowding could be predicted by integrating individual pre-tDCS behavioral performance and tDCS electric field simulation result. Approximately 66% of the variance in post-tDCS performance in the bipolar and HD-tDCS groups was explained by these two factors. Furthermore, the prediction model developed here was found to be generalizable to other two protocols with a different electrode size or a stimulation intensity. To our knowledge, this is the first model integrating pre-tDCS behavioral performance and electric field focality to

predict the effects of multiple tDCS protocols on post-tDCS behavioral performance.

Generally, tDCS studies using the double-blind design would be more reliable. In the current study, we assigned each subject to one of the five tDCS groups before the start of the experiment. The experiment consisted of three phases (i.e. pre-tDCS test, offline tDCS, and post-tDCS test), which took each subject about 1.5–2 continuous hours. The subject's performance data was transferred from the experiment computer to the data analysis computer after the three phases. Since we did not know subjects' performance before tDCS, it is very close to a double-blind design. In this way, we eliminated the experimenter bias in the single-blind experiment.

Our behavioral results revealed that protocols using HD-tDCS (at 1 mA or 2 mA) could significantly alleviate the visual crowding effect, while protocols using bipolar tDCS (with either 25 cm^2 or 8 cm^2 electrodes) could not. According to the simulation results based on sophisticated electrode and realistic head models, the HD-tDCS protocols constrained the electric field in less brain areas by positioning four returning electrodes around the stimulation electrode. Obviously, the HD-tDCS is more focal and possible to avoid activating brain regions irrelevant to crowding effect. We speculate that the HD-tDCS protocols are more effective than bipolar protocols in modulating neural activity in early visual cortex—i.e. activity that is closely associated with the visual crowding effect [33–36]. It should be noted that this claim is based on group-level results. It ignores the influence of non-optimal targeting on individual-level modulatory effects, as well as the resulting low- and non-responders. Theoretically, there should be some optimal tDCS montage specially targeting on the related brain region for each subject to alleviate individual visual crowding effect. Here, as a pre-step for future development of the optimized tDCS protocols, we proposed a model that could successfully predict the effects of tDCS at the individual level. The model made continuous predictions of subjects' post-tDCS orientation discrimination thresholds. In addition, our proposed model provides a comprehensive explanation of the causes of inter-individual variability in post-tDCS performance. Further study of the effects specified in our model may help guide the tuning required for individualized tDCS protocols. For example, the positive weight of the focality factor in the prediction model highlights the necessity of exploiting algorithms aiming at optimizing electrode placement and current dosage to maximize stimulation focality [49, 50].

It is worth noting that, in order to verify the simulation results of the current study, we compared the electric field distribution pattern and peak electric field strength with previous studies [1, 51, 52]. The HD-tDCS simulation results were consistent with a modeling study using similar montage and stimulation intensity [1]. Furthermore, our simulation results were comparable with a previous direct measurement study by Huang *et al*, which showed a peak electric field strength of 0.4 V m^{-1} for 1 mA stimulation and 0.8 V m^{-1} for 2 mA stimulation [52].

To date, the field strength necessary to modulate neuronal activity is still controversial. The strength of the tDCS-induced electric fields necessary to modulate neuronal activity depends on various factors, including the specific area of the brain being stimulated, the type of neurons being targeted, and the frequency and duration of the stimulation. Evidence derived from animal models suggests that the electric field threshold for neural activation is in the range of 0.2 V m^{-1}–0.5 V m^{-1} [53–57]. Even electric fields as weak as 0.2 V m^{-1} can have an impact on neural recordings [55], and the potential mechanism of such low-intensity electrical stimulation was explained by the changes in spike probability and timing [56, 58]. However, conclusions from animal models are based on brain slices or neural assemblies targeted by intracranial electrodes, and may not be directly generalizable for human studies [44]. Recently, Kasten *et al* used electric field modeling and neuroimaging to explain the variability of transcranial alternating current stimulation effects, and they showed that the electric field strength necessary to elicit stimulation effects in humans may be smaller than the thresholds estimated using animal models [44]. Accordingly, we defined electric field focality by assuming the electric field threshold in humans to be 0.1 V m^{-1}. Our results demonstrate that the focality factor defined here is a significant predictor of the modulatory effect on visual crowding.

The objective of our study was to develop a prediction model suitable for the most commonly used tDCS protocols (bipolar-25 tDCS and HD-1 mA tDCS). The proposed model enabled us to predict the post-tDCS performance based on a subject's pre-tDCS behavioral performance and head model. Additionally, the model based on the commonly used tDCS protocols was found to be transferable to the other two protocols using different electrode sizes or different stimulation intensities (bipolar-8 and HD-2 mA tDCS). Notably, when the model was applied to the data from the bipolar-8 and HD-2 mA tDCS groups, the form of the prediction model and the coefficients of each predictor were the same as those generated from the training. Compared to a model that only retains the form of the prediction model but regenerates the coefficients of the predictors and the constant term with new data, the model generalization test in our study was more stringent and provided greater practical value. In terms of the sample size of each tDCS group, it was determined based on

previous tDCS studies that have examined the effects on cognition [20, 32, 59, 60]. Moreover, the effect sizes of HD-tDCS on visual crowding, as well as the proposed model on predicting the post-tDCS performance, were moderate to strong.

Our study provides the first tests of the model's prediction performance in multiple tDCS protocols. The generalizability analysis showed that our model could capably predict the variability in post-tDCS performance of the bipolar-8 tDCS group. However, for the 2 mA HD-tDCS group, our model explained only 40% of the variance in post-tDCS performance. We speculate that the weaker performance for the HD-2 mA tDCS protocol is due to a nonlinear relationship between stimulation intensity and tDCS effect. Accordingly, tDCS-induced facilitation of cortical excitability may be due to synaptic mechanisms associated with long-term potentiation [61]. Increasing stimulation intensity therefore does not necessarily enhance tDCS effects [61–66]. Thus, when directly generalizing a linear model developed using data from the 1 mA tDCS group to the 2 mA tDCS group, the model's performance was barely satisfactory. Moreover, one limitation regarding the prediction model in this case is the definition of the stimulation-induced electric field, which is based on the normal value of the electric field and ignores its relative direction to the cortical surface. Previous work has demonstrated that perpendicular and parallel components of the electric field might contribute differently to the stimulation effects [67]. Future work may incorporate these components into a regression model to investigate their effects on the visual crowding task. In addition, despite significantly predicting the effects of different tDCS protocols on visual crowding, whether the proposed model will still work well for other cognitive tasks remains unknown. Future work should assess the generalizability of our model for different tasks.

5. Conclusion

tDCS has shown great promise in enhancing brain function. Considerable research has focused on identifying reliable and stable stimulation protocols that could be applied for clinical uses [68–70]. Identifying the key factors determining the effects of tDCS is crucial for the design of individualized stimulation protocols. In the current work, we propose an efficient model that can reinforce our understanding of the contribution of individual pre-tDCS behavioral performance and electric field distribution on the variability in inter-individual tDCS outcomes. This data may help define the objective function for target optimization when multiple electrodes are used for individualized tDCS protocols, and this in turn may have implications for future experimental and therapeutic tDCS applications.

Data availability statements

All data that support the findings of this study are included within the article (and any supplementary files).

Acknowledgments

This study was supported by the National Science and Technology Innovation 2030 Major Program (2022ZD0204802), the National Key R&D Program of China (2020AAA0105200), the National Natural Science Foundation of China (31930053), and Beijing Academy of Artificial Intelligence (BAAI).

Conflict of interests

The authors declare no competing interests.

Author contributions

Chen Luyao: Conceptualization, Methodology, Data curation, Writing-Original draft preparation. Chen Guanpeng: Investigation, Writing-Reviewing and Editing. Gong Xizi: Validation, Investigation, Writing-Reviewing and Editing. Fang Fang: Conceptualization, Supervision, Writing-Reviewing and Editing.

ORCID iD

Luyao Chen https://orcid.org/0000-0001-6048-9985

References

[1] Datta A, Bansal V, Diaz J, Patel J, Reato D and Bikson M 2009 Gyri-precise head model of transcranial direct current stimulation: improved spatial focality using a ring electrode versus conventional rectangular pad *Brain Stimul.* **2** 201–207.e1

[2] Edwards D, Cortes M, Datta A, Minhas P, Wassermann E M and Bikson M 2013 Physiological and modeling evidence for focal transcranial electrical brain stimulation in humans: a basis for high-definition tDCS *NeuroImage* **74** 266–75

[3] Kuo H I, Bikson M, Datta A, Minhas P, Paulus W, Kuo M F and Nitsche M A 2013 Comparing cortical plasticity induced by conventional and high-definition 4 × 1 ring tDCS: a neurophysiological study *Brain Stimul.* **6** 644–8

[4] Arul-Anandam A P and Loo C 2009 Transcranial direct current stimulation: a new tool for the treatment of depression? *J. Affective Disorders* **117** 137–45

[5] Baker J M, Rorden C and Fridriksson J 2010 Using transcranial direct-current stimulation to treat stroke patients with aphasia *Stroke* **41** 1229–36

[6] Yu Y, Fan Y, Han F, Luan G and Wang Q 2023 Transcranial direct current stimulation inhibits epileptic activity propagation in a large-scale brain network model *Sci. China Technol. Sci.* (https://doi.org/10.1007/s11431-022-2341-x)

[7] Mosayebi Samani M, Agboada D, Jamil A, Kuo M F and Nitsche M A 2019 Titrating the neuroplastic effects of

cathodal transcranial direct current stimulation (tDCS) over the primary motor cortex *Cortex* **119** 350–61
[8] Paracampo R, Montemurro M, de Vega M and Avenanti A 2018 Primary motor cortex crucial for action prediction: a tDCS study *Cortex* **109** 287–302
[9] Yang X, He Q and Fang F 2022 Transcranial direct current stimulation over the visual cortex facilitates awake consolidation of visual perceptual learning *Brain Stimul.* **15** 380–2
[10] Antal A and Paulus W 2008 Transcranial direct current stimulation and visual perception *Perception* **37** 367–74
[11] Flöel A 2014 tDCS-enhanced motor and cognitive function in neurological diseases *NeuroImage* **85** 934–47
[12] Reinhart R M G, Xiao W, McClenahan L J and Woodman G F 2016 Electrical stimulation of visual cortex can immediately improve spatial vision *Curr. Biol.* **26** 1867–72
[13] Martin A K, Huang J, Hunold A and Meinzer M 2019 Dissociable roles within the social brain for self–other processing: a HD-tDCS study *Cereb. Cortex* **29** 3642–54
[14] Filmer H L, Mattingley J B and Dux P E 2020 Modulating brain activity and behaviour with tDCS: rumours of its death have been greatly exaggerated *Cortex* **123** 141–51
[15] Jonker Z D, Gaiser C, Tulen J H M, Ribbers G M, Frens M A and Selles R W 2021 No effect of anodal tDCS on motor cortical excitability and no evidence for responders in a large double-blind placebo-controlled trial *Brain Stimul.* **14** 100–9
[16] Kim J H, Kim D W, Chang W H, Kim Y H, Kim K and Im C H 2014 Inconsistent outcomes of transcranial direct current stimulation may originate from anatomical differences among individuals: electric field simulation using individual MRI data *Neurosci. Lett.* **564** 6–10
[17] de Aguiar V *et al* 2020 Cognitive and language performance predicts effects of spelling intervention and tDCS in primary progressive aphasia *Cortex* **124** 66–84
[18] Hill A T, Rogasch N C, Fitzgerald P B and Hoy K E 2019 Impact of concurrent task performance on transcranial direct current stimulation (tDCS)-induced changes in cortical physiology and working memory *Cortex* **113** 37–57
[19] Martin D M, Yeung K and Loo C K 2016 Pre-treatment letter fluency performance predicts antidepressant response to transcranial direct current stimulation *J. Affective Disorders* **203** 130–5
[20] McConathey E M, White N C, Gervits F, Ash S, Coslett H B, Grossman M and Hamilton R H 2017 Baseline performance predicts tDCS-mediated improvements in language symptoms in primary progressive aphasia *Front. Hum. Neurosci.* **11** 347
[21] Mahdavi S and Towhidkhah F 2018 Computational human head models of tDCS: influence of brain atrophy on current density distribution *Brain Stimul.* **11** 104–7
[22] Opitz A, Paulus W, Will S, Antunes A and Thielscher A 2015 Determinants of the electric field during transcranial direct current stimulation *NeuroImage* **109** 140–50
[23] Schmidt C, Wagner S, Burger M, van Rienen U and Wolters C H 2015 Impact of uncertain head tissue conductivity in the optimization of transcranial direct current stimulation for an auditory target *J. Neural Eng.* **12** 046028
[24] Shahid S, Wen P and Ahfock T 2013 Numerical investigation of white matter anisotropic conductivity in defining current distribution under tDCS *Comput. Methods Programs Biomed.* **109** 48–64
[25] Suh H S, Lee W H and Kim T S 2012 Influence of anisotropic conductivity in the skull and white matter on transcranial direct current stimulation via an anatomically realistic finite element head model *Phys. Med. Biol.* **57** 6961–80
[26] Cotelli M *et al* 2016 Grey matter density predicts the improvement of naming abilities after tDCS intervention in agrammatic variant of primary progressive aphasia *Brain Topogr.* **29** 738–51
[27] Zhao Y, Ficek B, Webster K, Frangakis C, Caffo B, Hillis A E, Faria A and Tsapkini K 2021 White matter integrity predicts electrical stimulation (tDCS) and language therapy effects in primary progressive aphasia *Neurorehabil. Neural Repair* **35** 44–57
[28] de Aguiar V *et al* 2020 Brain volumes as predictors of tDCS effects in primary progressive aphasia *Brain Lang.* **200** 104707
[29] Whitney D and Levi D M 2011 Visual crowding: a fundamental limit on conscious perception and object recognition *Trends Cogn. Sci.* **15** 160–8
[30] Levi D M 2008 Crowding—an essential bottleneck for object recognition: a mini-review *Vis. Res.* **48** 635–54
[31] Hussain Z, Webb B S, Astle A T and McGraw P V 2012 Perceptual learning reduces crowding in amblyopia and in the normal periphery *J. Neurosci.* **32** 474–80
[32] Chen G, Zhu Z, He Q and Fang F 2021 Offline transcranial direct current stimulation improves the ability to perceive crowded targets *J. Vis.* **21** 1
[33] Bi T, Cai P, Zhou T and Fang F 2009 The effect of crowding on orientation-selective adaptation in human early visual cortex *J. Vis.* **9** 13
[34] Chen J, He Y, Zhu Z, Zhou T, Peng Y, Zhang X and Fang F 2014 Attention-dependent early cortical suppression contributes to crowding *J. Neurosci.* **34** 10465–74
[35] He D, Wang Y and Fang F 2019 The critical role of V2 population receptive fields in visual orientation crowding *Curr. Biol.* **29** 2229–36.e3
[36] Millin R, Arman A C, Chung S T L and Tjan B S 2014 Visual crowding in V1 *Cereb. Cortex* **24** 3107–15
[37] Ai H and Chen N 2020 The crowded window of object recognition revealed by cortical population codes *Sci. China Life Sci.* **63** 317–8
[38] Watson A B and Pelli D G 1983 Quest: a Bayesian adaptive psychometric method *Percept. Psychophys.* **33** 113–20
[39] Windhoff M, Opitz A and Thielscher A 2013 Electric field calculations in brain stimulation based on finite elements: an optimized processing pipeline for the generation and usage of accurate individual head models *Hum. Brain Mapp.* **34** 923–35
[40] Thielscher A, Antunes A and Saturnino G B 2015 Field modeling for transcranial magnetic stimulation: a useful tool to understand the physiological effects of TMS? *2015 37th Annual Int. Conf. IEEE Engineering in Medicine and Biology Society (EMBC) (10 May 2023)* (IEEE) pp 222–5 (available at: http://ieeexplore.ieee.org/document/7318340/)
[41] Wagner T A, Zahn M, Grodzinsky A J and Pascual-Leone A 2004 Three-dimensional head model simulation of transcranial magnetic stimulation *IEEE Trans. Biomed. Eng.* **51** 1586–98
[42] Turnbull A, Anthony M, Tadin D, Porsteinsson A P, Heffner K and Lin F V 2023 Effect of online tDCS to left somatomotor cortex on neuropsychiatric symptoms among older adults at risk for dementia *Cortex* **159** 131–41
[43] Antonenko D, Grittner U, Saturnino G, Nierhaus T, Thielscher A and Flöel A 2021 Inter-individual and age-dependent variability in simulated electric fields induced by conventional transcranial electrical stimulation *NeuroImage* **224** 117413
[44] Kasten F H, Duecker K, Maack M C, Meiser A and Herrmann C S 2019 Integrating electric field modeling and neuroimaging to explain inter-individual variability of tACS effects *Nat. Commun.* **10** 5427
[45] Glasser M F *et al* 2016 A multi-modal parcellation of human cerebral cortex *Nature* **536** 171–8
[46] Fischl B, Sereno M I, Tootell R B H and Dale A M 1999 High-resolution intersubject averaging and a coordinate system for the cortical surface *Hum. Brain Mapp.* **8** 272–84
[47] Fischl B, Sereno M I and Dale A M 1999 Cortical surface-based analysis: II. Inflation, flattening, and a surface-based coordinate system *NeuroImage* **9** 195–207
[48] Dale A M, Fischl B and Sereno M I 1999 Cortical surface-based analysis: I. Segmentation and surface reconstruction *NeuroImage* **9** 179–94

[49] Dmochowski J P, Datta A, Bikson M, Su Y and Parra L C 2011 Optimized multi-electrode stimulation increases focality and intensity at target *J. Neural Eng.* **8** 046011
[50] Guler S, Dannhauer M, Erem B, Macleod R, Tucker D, Turovets S, Luu P, Erdogmus D and Brooks D H 2016 Optimization of focality and direction in dense electrode array transcranial direct current stimulation (tDCS) *J. Neural Eng.* **13** 036020
[51] Faria P, Hallett M and Miranda P C 2011 A finite element analysis of the effect of electrode area and inter-electrode distance on the spatial distribution of the current density in tDCS *J. Neural Eng.* **8** 066017
[52] Huang Y, Liu A A, Lafon B, Friedman D, Dayan M, Wang X, Bikson M, Doyle W K, Devinsky O and Parra L C 2017 Measurements and models of electric fields in the in vivo human brain during transcranial electric stimulation *eLife* **6** e18834
[53] Antal A and Herrmann C S 2016 Transcranial alternating current and random noise stimulation: possible mechanisms *Neural Plast.* **2016** 1–12
[54] Fröhlich F and McCormick D A 2010 Endogenous electric fields may guide neocortical network activity *Neuron* **67** 129–43
[55] Jackson M P, Rahman A, Lafon B, Kronberg G, Ling D, Parra L C and Bikson M 2016 Animal models of transcranial direct current stimulation: methods and mechanisms *Clin. Neurophysiol.* **127** 3425–54
[56] Reato D, Rahman A, Bikson M and Parra L C 2010 Low-intensity electrical stimulation affects network dynamics by modulating population rate and spike timing *J. Neurosci.* **30** 15067–79
[57] Chase H W, Boudewyn M A, Carter C S and Phillips M L 2020 Transcranial direct current stimulation: a roadmap for research, from mechanism of action to clinical implementation *Mol. Psychiatry* **25** 397–407
[58] Liu A *et al* 2018 Immediate neurophysiological effects of transcranial electrical stimulation *Nat. Commun.* **9** 5092
[59] Antal A, Nitsche M A, Kruse W, Kincses T Z, Hoffmann K P and Paulus W 2004 Direct current stimulation over V5 enhances visuomotor coordination by improving motion perception in humans *J. Cogn. Neurosci.* **16** 521–7
[60] Wu D, Li C, Liu N, Xu P and Xiao W 2020 Visual motion perception improvements following direct current stimulation over V5 are dependent on initial performance *Exp. Brain Res.* **238** 2409–16
[61] Kidgell D J, Daly R M, Young K, Lum J, Tooley G, Jaberzadeh S, Zoghi M and Pearce A J 2013 Different current intensities of anodal transcranial direct current stimulation do not differentially modulate motor cortex plasticity *Neural Plast.* **2013** 1–9
[62] Ammann C, Lindquist M A and Celnik P A 2017 Response variability of different anodal transcranial direct current stimulation intensities across multiple sessions *Brain Stimul.* **10** 757–63
[63] Batsikadze G, Moliadze V, Paulus W, Kuo M F and Nitsche M A 2013 Partially non-linear stimulation intensity-dependent effects of direct current stimulation on motor cortex excitability in humans: effect of tDCS on cortical excitability *J. Physiol.* **591** 1987–2000
[64] Benwell C S Y, Learmonth G, Miniussi C, Harvey M and Thut G 2015 Non-linear effects of transcranial direct current stimulation as a function of individual baseline performance: evidence from biparietal tDCS influence on lateralized attention bias *Cortex* **69** 152–65
[65] Esmaeilpour Z, Marangolo P, Hampstead B M, Bestmann S, Galletta E, Knotkova H and Bikson M 2018 Incomplete evidence that increasing current intensity of tDCS boosts outcomes *Brain Stimul.* **11** 310–21
[66] Jamil A, Batsikadze G, Kuo H I, Labruna L, Hasan A, Paulus W and Nitsche M A 2017 Systematic evaluation of the impact of stimulation intensity on neuroplastic after-effects induced by transcranial direct current stimulation: effects of DC intensity on cortical excitability *J. Physiol.* **595** 1273–88
[67] Rahman A, Reato D, Arlotti M, Gasca F, Datta A, Parra L C and Bikson M 2013 Cellular effects of acute direct current stimulation: somatic and synaptic terminal effects: somatic and terminal origin of DCS effects *J. Physiol.* **591** 2563–78
[68] Ahn S, Mellin J M, Alagapan S, Alexander M L, Gilmore J H, Jarskog L F and Fröhlich F 2019 Targeting reduced neural oscillations in patients with schizophrenia by transcranial alternating current stimulation *NeuroImage* **186** 126–36
[69] Kekic M, Boysen E, Campbell I C and Schmidt U 2016 A systematic review of the clinical efficacy of transcranial direct current stimulation (tDCS) in psychiatric disorders *J. Psychiatry Res.* **74** 70–86
[70] Mellin J M, Alagapan S, Lustenberger C, Lugo C E, Alexander M L, Gilmore J H, Jarskog L F and Fröhlich F 2018 Randomized trial of transcranial alternating current stimulation for treatment of auditory hallucinations in schizophrenia *Eur. Psychiatry* **51** 25–33